CETRA2022 11-13 May 2022, Pula, Croatia
7th International Conferenceon Road and Rail Infrastructure

INTEGRATED FIBER BRAGG GRATING SENSOR FOR BRIDGE LOAD MEASUREMENT AND TRAFFIC LOAD ESTIMATION

Jan Včelák[1, 2], Jakub Vaněk[2], Emil Doupal[3], Miroslav Juhas[4]
[1] *InnoRenew CoE, Slovenia*
[2] *Czech Technical University in Prague, University Centre for Energy Efficient Buildings, Czech Republic*
[3] *Transport Research Centre, Czech Republic*
[4] *Camea Technology a.s., Czech Republic*

Abstract

Condition of road bridges in central as well as eastern Europe is not excellent. Lack of funding for maintenance requires precise identification of road bridge in need of investment. Integration of permanent monitoring sensors during construction of new bridge is a tool for integrated diagnostics. While the integrated Fiber Bragg Grating (FBG) sensors can be used for strain measurement or crack detection, in meantime they could be the same sensors used for traffic load estimation. Two types of FBG sensors were installed in concrete road bridge during construction phase in 2017 Czech Republic. Two FBG sensors in steel body and 4 Glass Fiber Reinforced Polymer GFRP sensor chain was integrated in the concrete body of the pre-stressed reinforced concrete element. Sensors are measuring strain in longitudinal direction of the bridge close to the bottom edge of the bridge where load on the bridge is causing extension. The signal from FBG sensors is processed by interrogation unit FBGuard and since they are embedded in the concrete, they are well protected against vandalism as well as against outdoor weather conditions. Weight in Motion (WIM) system together with measurement of acceleration was installed on the same bridge element as a reference system for accurate identification of vehicle type, speed, axle load measurement and bridge deflection under vehicles passed over the bridge element. Methods of fiber optic sensor (FOS) signal processing, mathematical processing to determine important traffic parameters, FOS system accuracy and reliability will be presented in this paper. Limitations of the system will be also discussed in the paper. Installed FOS system is used to determine vehicle number, speed, and weight estimation. Results of signal processing and calculation of traffic parameters from FOS system will be shown on real data obtained from the bridge load tests carried out in 2021.

Keywords: road bridge monitoring, traffic monitoring, optic fiber sensors

1 Introduction

Structural health monitoring of road bridges is a sensor system application which is still not a common tool to provide predictive maintenance plan or detect any dangerous situations related to aging, periodic overloading or any other effect to which the bridge is exposes to during normal operation. Most of the road bridge constructions are made from steel, reinforced concrete or rarely from timber. Bridge and tunnels are expensive parts of road or railway infrastructure and therefore any aim to extend the operation period or

DOI: https://doi.org/10.5592/CO/CETRA.2022.1350

regular maintenance periods means substantial cost savings and increasing the safety of the infrastructure.

The load of the road bridges caused by traffic can be well estimated using weight in motion (WIM). In past projects it has been shown that dedicated Bridge-Weight in motion (BWIM) sensors are able to reliably detect oversized, overweight vehicles, speed exceeding on the road bridges [2]. While the load from traffic is able to be determined from a BWIM systems consequences of long-term exposure to outdoor environment conditions, natural aging, consequences of chemical road treatments, or structural failures are hard to be predicted since they do not need to have immediate visible results. Therefore it is convenient to combine BWIM and Structural health monitoring (SHM) systems both together, to have complete overview of the bridge behavior and influences. Traditional BWIM systems require axle detecting sensors (tape switch or piezoelectric sensors, induction loops) mounted in the top layer of the road. Such sensors require expensive installation in the paved layer and have limited operational life. "Free of axle detector" (FAD) BWIM systems use load measurement usually inside the structure or at the bottom part of the bridge element to estimate what was the weight and speed of the vehicle causing the load. FAD BWIM systems are described in [1, 5] together with load responses in strain from the truck vehicle.

First basic concepts of BWIM systems were developed and verified by Moses [3] and they using instrumented bridge as a sensor with mounted sensors on the soffit. Most of the BWIM systems are based on the influence line estimation because this is one of the crucial parameters which describes the bridge behavior under the traffic load [1-3, 5]. Theoretically calculated IL does not always represent the bridge behavior and calibration procedures are required [1].

Most of the BWIM systems use dedicated sensors that are needed to be installed after the bridge is completed. In this paper we would like to present new approach where sensors originally planned for structural health monitoring (SHM) are used as BWIM system. The sensors are integrated directly in the concrete structure and thus are protected and hidden from ambient conditions. On the other hand the sensors installed for SHM requires different location then standard sensors for BWIM system.

Fibre optic sensors (FOS) can be used to monitor several parameters of the civil engineering structures [9]. The capabilities of FOS sensors are covering monitoring of temperature, moisture, strain, pH value, corrosion, carbon dioxide, chlorides as shown in [9]. In case of SHM sensing for a concrete road bridge FOS can sense load, strain or temperature values of the bridge elements [7]. The FOS in a form of GRFP string can be used with advantage because string type of Fibre Brag Grating (FBG) can contain many sensors in a single string and is ideal for monitoring linear infrastructure elements. The position of the sensor in the longitudinal direction of the infrastructure element is not ideal for axle load, or speed sensing. The FOS sensors can be used for timber elements from glulam and also for reinforced concrete bridge elements as shown in [7]. The main advantage of the integrated FOS sensors is the fact that are fully integrated in the structural element and thus not exposed to harsh environmental conditions, mechanical damages or vandalism. SHM sensors are not used intensively, only time to time for periodic checks and most of the time they are not acquiring any data. Therefore FOS can be used for other purposes then SHM in the same time. One of the possible application of already installed FOS sensors would be traffic monitoring. More about principles FBG sensors can be found in [11].

Even if the SHM sensors are not ideal for BWIM implementation it is possible to estimate traffic load with limited accuracy and limited reliability. In this paper we will present the achievable accuracies of vehicle speed, count and weight estimation by using SHM FOS sensors installed in the reinforced pre-stressed concrete bridge. The accuracy of developed algorithms will be shown on real gathered data from the monitored road bridge in Stare Hobzi, Czech Republic.

2 Sensor installation and system

2.1 Optical sensor system

FBG sensors were installed during construction of a new road bridge in southern part of Czech Republic in 2017. Primary goal of the sensor installation was Structural Health Monitoring (SHM) of reinforced pre-stressed concrete bridge spans of length 23, 30 and 23 m. The width is 8.5 m and depth varies from 1.0 m in the middle to 1.6 m above the supports (see Figure 1) [7]. Two different types of FOS sensors were installed into the first bridge span (see Figure 1 and Weight error 7 % (category B+(7) from COST 323 [13]):

- Two FBG sensor in Glass Fiber Reinforced Polymer (GFRP) string with outer diameter 1 [7]
- Two Embedded Strain FBG sensors. Installed on steel rebars. Strain sensitivity 1.2, fiber type SMF G.652. Made by Safibra [10].

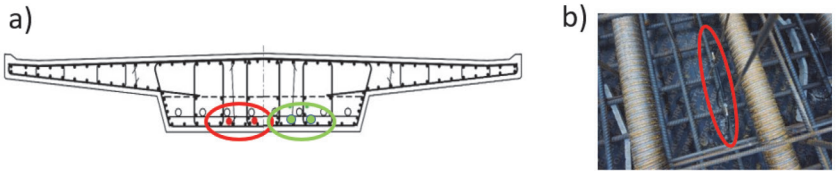

Figure 1 Shematic cross section of bridge structure: a) Red dots are two Embeeded sensors and its positions b) Green dots are Gfrp sensors [7]

Data from FOS sensors are acquired using interrogation unit called FBGuard 1550 from Safibra [10]. Unit uses light source with wavelength range from 1550 to 1590. Wavelength resolution of interrogator unit is ≤ 1 and wavelength repeatability ± 5. The maximal scan frequency depends on number of used channels. For 1 channel is up to 11 kHz, 1 kHz at 2 channels and 125 Hz at 16 channels [7, 10].

2.2 WIM system

Reference Weight-in-motion (WIM) system from Camea [12] system was installed for traffic statistics evaluation. WIM is installed just before first bridge span (see Weight error 7 % (category B+(7) from COST 323 [13]).). For our WIM configuration manufacturer declares [12]:

- Speed error 2 km/h
- Length error 1 cm or 1 % of length
- Weight error 7 % (category B+(7) from COST 323 [13]).

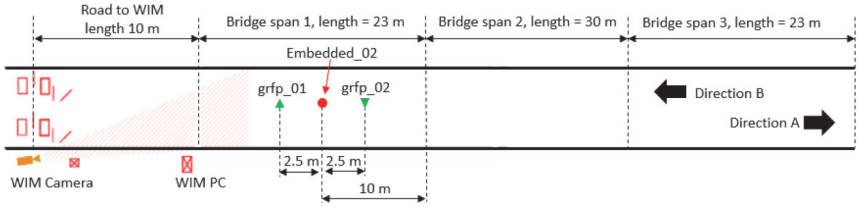

Figure 2 Location of WIM and optical sensors

3 Data processing

FOS data were collected in one day using two calibrated trucks with known axle weight and length. The sample rate of FOS data acquisition was set to 10 Hz which corresponds to sampling period T=100 ms.
The FOS sensors are located in the first span and measure strain in longitudinal direction (see Figure 1 and Weight error 7 % (category B+(7) from COST 323 [13]).). Three peaks are visible during a vehicle passage over the bridge (see Three peaks are visible during a vehicle passage over the bridge (see Three peaks are visible during a vehicle passage over the bridge (see Figure 3). Each corresponds to a passage through one bridge span. The most significant peak to positive values and its amplitude εpeakup corresponds to the span in which the sensors are located. The second most significant peak (εpeakdown), with negative amplitude, corresponds to the middle bridge span. The third and smallest peak with positive amplitude corresponds to the last span. The third peak may not be detectable for lighter vehicles.). Each corresponds to a passage through one bridge span. The most significant peak to positive values and its amplitude εpeakup corresponds to the span in which the sensors are located. The second most significant peak (εpeakdown), with negative amplitude, corresponds to the middle bridge span. The third and smallest peak with positive amplitude corresponds to the last span. The third peak may not be detectable for lighter vehicles.). Each corresponds to a passage through one bridge span. The most significant peak to positive values and its amplitude εpeakup corresponds to the span in which the sensors are located. The second most significant peak (εpeakdown), with negative amplitude, corresponds to the middle bridge span. The third and smallest peak with positive amplitude corresponds to the last span. The third peak may not be detectable for lighter vehicles. shows typical FOS signal pattern during the passage of the vehicle over the bridge. Because the original purpose of FOS sensor installation is SHM and not detection of traffic, it is not possible to detect the passage of individual axles from the signal. The original measured signal is shown in black in Three peaks are visible during a vehicle passage over the bridge (see Three peaks are visible during a vehicle passage over the bridge (see Three peaks are visible during a vehicle passage over the bridge (see Figure 3). Each corresponds to a passage through one bridge span. The most significant peak to positive values and its amplitude εpeakup corresponds to the span in which the sensors are located. The second most significant peak (εpeakdown), with negative amplitude, corresponds to the middle bridge span. The third and smallest peak with positive amplitude corresponds to the last span. The third peak may not be detectable for lighter vehicles.). Each corresponds to a passage through one bridge span. The most significant peak to positive values and its amplitude εpeakup corresponds to the span in which the sensors are located. The second most significant peak (εpeakdown), with negative amplitude, corresponds to the middle bridge span. The third and smallest peak with positive amplitude corresponds to the last span. The third peak may not be detectable for lighter vehicles.). Each corresponds to a passage through one bridge span. The most significant peak to positive values and its amplitude εpeakup corresponds to the span in which the sensors are located. The second most significant peak (εpeakdown), with negative amplitude, corresponds to the middle bridge span. The third and smallest peak with positive amplitude corresponds to the last span. The third peak may not be detectable for lighter vehicles..
The FOS signal is first processed by a moving average filter using window of 25 samples to remove signal noise. Various types of more sophisticated filters have also been tested (Butterworth and Chebyshev), but the moving average has proven to be a robust enough option for this situation, fully meeting the noise elimination requirements. The filtered signal is highlighted in red.

Three peaks are visible during a vehicle passage over the bridge (see Three peaks are visible during a vehicle passage over the bridge (see Three peaks are visible during a vehicle passage over the bridge (see Figure 3). Each corresponds to a passage through one bridge span. The most significant peak to positive values and its amplitude εpeakup corresponds to the span in which the sensors are located. The second most significant peak (εpeakdown), with negative amplitude, corresponds to the middle bridge span. The third and smallest peak with positive amplitude corresponds to the last span. The third peak may not be detectable for lighter vehicles.). Each corresponds to a passage through one bridge span. The most significant peak to positive values and its amplitude εpeakup corresponds to the span in which the sensors are located. The second most significant peak (εpeakdown), with negative amplitude, corresponds to the middle bridge span. The third and smallest peak with positive amplitude corresponds to the last span. The third peak may not be detectable for lighter vehicles.). Each corresponds to a passage through one bridge span. The most significant peak to positive values and its amplitude ε_{peakup} corresponds to the span in which the sensors are located. The second most significant peak ($\varepsilon_{peakdown}$), with negative amplitude, corresponds to the middle bridge span. The third and smallest peak with positive amplitude corresponds to the last span. The third peak may not be detectable for lighter vehicles.

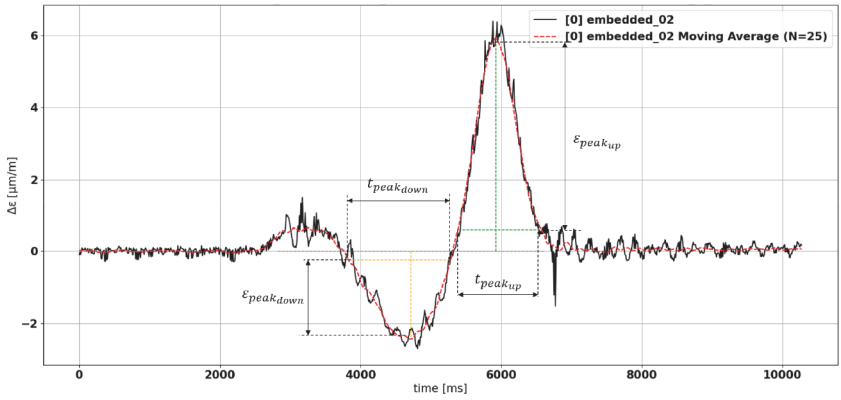

Figure 3 FOS signal pattern - Passage of one vehicle in direction B

3.1 Method for speed calculations

All strain parameters of the peak are related relative to the idle (no load) value . The highest peak in the data is identified first from one passage. The peak strain amplitude value is ε_{imax} and its index i_{max} related to the beginning of the processed passage. The duration of the peak is determined by the indexes i_{start} and i_{end}. These indexes are determined by the points at which the following conditions are met:

$$\left|\varepsilon_{i_{start}}\right| \leq \left|\varepsilon_{max} / 10\right| \quad (1)$$

$$\left|\varepsilon_{i_{end}}\right| \leq \left|\varepsilon_{max} / 10\right| \quad (2)$$

At the same time, condition (1) must be met for 50 % of the previous 100 values. Similarly, condition (2) for the following values. These additional conditions are used to filter oscillations / noise around the idle value. The duration of the peak is then given by:

$$t = (i_{end} - i_{start}) \cdot T \quad (3)$$

A similar method is used to identify the second most remarkable peak, which is additionally supplemented by the condition that it must be before / after the largest peak. The duration of the peak t and the known length of the span or spans field d to which the peak belongs are used to calculate the speed v.

$$e_a = v_{WIM} - v_{sensor} \tag{4}$$

where e_a [km/h] is absolute speed error, v_{WIM} speed acquired by WIM system (referent speed for us), v_{sensor} calculated speed from any our sensor.

Following formula is used to calculate relative speed error:

$$e_r = \frac{|v_{WIM} - v_{sensor}|}{v_{WIM}} \tag{5}$$

where e_r [%] is relative speed error.

4 Results

All comparisons given bellow are related to installed WIM system which is taken as a reference measurement. Authors are aware that WIM has its own precision which may cause additional errors.

4.1 Speed calculations

Vehicles are divided into three categories for the purpose of statistical processing:
- Trucks (calibration truck) – testing vehicles of known axle-weight (total weight 17800 and 18390 kg), total length (16.3 and 17.5 m) and axles spacing (5 axles). Measured before test.
- Other heavy – group of heavy vehicles - weight, speed and length measured by WIM
- Cars – group of light vehicles - weight, speed and length measured by WIM.

Case specific parameters are used for speed calculations:
- Case S1: Length of first bridge span which is 23 m and duration of peak up corresponding with vehicle passing first span is used.
- Case S2: Lengths (lengths of first and second bridge spans) and corresponding times are used.
- Case S3: Length and duration is used for speed calculation. Result speed is then corrected by linear regression calculated separately for each category.
- Case S4: Length of first bridge span and which is length of vehicle provided by WIM system is used. Duration is then used for speed calculation. Speed is then corrected by linear regression. Regression coefficients are calculated separately for each category of vehicles.

For results of measurement see For results of measurement see For results of measurement see Table 1. Mean errors, standard deviations (SD) and variances (VAR) are presented. “All” category summarizes results of all data. Mean errors, standard deviations (SD) and variances (VAR) are presented. “All” category summarizes results of all data. Mean errors, standard deviations (SD) and variances (VAR) are presented. “All” category summarizes results of all data.

Table 1 Comparison of speed absolute and relative speed errors

Case	Category	Embedded_02						gfrp_01						gfrp_02					
		Absolute error [km/h]			Relative error [%]			Absolute error [km/h]			Relative error [%]			Absolute error [km/h]			Relative error [%]		
		MEAN	SD	VAR	MEAN	SD	VAR	MEAN	SD	VAR	MEAN	SD	VAR	MEAN	SD	VAR	MEAN	SD	VAR
S1	Trucks	5.8	3.5	12.5	10.7	5.6	31.7	6.9	4.6	21.4	14.3	5.7	32.5	2.9	4.4	19.6	8.2	4.1	17.2
	Other heavy	-1.0	6.4	41.3	7.8	7.2	51.8	1.8	5.4	28.7	6.9	8.2	67.1	-4.3	7.1	50.2	11.0	5.0	24.7
	Cars	-7.9	4.9	24.4	10.1	5.5	30.7	-5.8	4.8	23.3	8.5	5.0	24.6	-12.3	6.6	43.5	14.7	7.1	50.6
	All	4.9	5.0	26.0	9.5	6.1	38.1	4.9	4.9	24.5	9.9	6.3	41.4	6.5	6.0	37.8	11.3	5.4	30.8
S2	Trucks	2.0	4.1	16.5	4.9	6.2	38.2	2.4	5.1	26.1	6.4	6.5	42.8	-0.3	2.3	5.5	3.3	2.5	6.4
	Other heavy	-2.7	5.0	25.0	7.5	4.4	19.7	-2.6	5.7	32.7	8.1	5.4	29.3	-4.4	4.8	23.2	8.7	4.4	19.1
	Cars	-7.8	5.6	31.0	10.5	5.4	29.3	-7.6	4.3	18.6	9.6	5.2	26.8	-9.8	4.4	19.8	11.9	5.6	31.3
	All	4.1	4.9	24.2	7.6	5.3	29.1	4.2	5.0	25.8	8.0	5.7	33.0	4.8	3.9	16.1	8.0	4.2	18.9
S3	Trucks	0.0	3.1	9.9	4.0	3.3	10.9	0.0	4.4	19.5	4.8	7.1	50.5	0.0	4.4	19.6	5.5	5.5	29.9
	Other heavy	0.0	6.1	37.3	6.8	6.6	44.1	0.0	5.5	30.1	6.8	5.5	30.3	0.0	6.4	41.1	7.3	6.6	43.6
	Cars	0.0	5.8	34.1	6.7	4.2	17.9	0.0	5.6	31.1	6.1	4.2	17.9	0.0	9.4	88.7	10.9	7.1	50.8
	All	0.0	5.0	27.1	5.8	4.7	24.3	0.0	5.2	26.9	5.9	5.6	32.9	0.0	6.8	49.8	7.9	6.4	41.4
S4	Trucks	0.0	3.3	10.8	4.3	3.1	9.4	0.0	4.5	19.9	4.7	5.2	27.4	0.0	4.5	19.9	5.5	4.8	22.8
	Other heavy	0.0	6.2	37.9	8.0	7.8	61.0	0.0	5.4	28.9	6.6	7.1	50.9	0.0	5.6	31.6	7.0	7.4	54.1
	Cars	0.0	5.0	25.4	5.6	4.8	22.7	0.0	5.5	30.7	5.4	5.6	31.6	0.0	7.7	59.2	9.1	5.4	28.9
	All	0.0	4.8	24.7	6.0	5.2	31.1	0.0	5.1	26.5	5.6	6.0	36.6	0.0	5.9	36.9	7.2	5.8	35.3

4.2 Weight measurement

Weight estimation is based on measurements of peak amplitudes () see Three peaks are visible during a vehicle passage over the bridge (see Three peaks are visible during a vehicle passage over the bridge (see Figure 3). Each corresponds to a passage through one bridge span. The most significant peak to positive values and its amplitude εpeakup corresponds to the span in which the sensors are located. The second most significant peak (εpeakdown), with negative amplitude, corresponds to the middle bridge span. The third and smallest peak with positive amplitude corresponds to the last span. The third peak may not be detectable for lighter vehicles.). Each corresponds to a passage through one bridge span. The most significant peak to positive values and its amplitude εpeakup corresponds to the span in which the sensors are located. The second most significant peak (εpeakdown), with negative amplitude, corresponds to the middle bridge span. The third and smallest peak with positive amplitude corresponds to the last span. The third peak may not be detectable for lighter vehicles.. Amplitude is recalculated to weight. This calculation is based on linear regression and known weight of vehicle obtained from WIM. WIM weight was used for system calibration, and it's not needed to be known for future calculations. Three different approaches were used:

- Case W1: amplitude of dominant is used.
- Case W2: amplitude of is used.
- Case W3: sum of amplitudes and is used.

Weight calculation results are compared in Weight calculation results are compared in Weight calculation results are compared in Table 2. All sensors have best results for method W1, which use only amplitude of peak up. Much more accurate results are achieved for heavy vehicles. Which is good news for practical application of the system because heavy vehicles can cause more structural damage.. All sensors have best results for method W1, which use only amplitude of peak up. Much more accurate results are achieved for heavy vehicles. Which is good news for practical application of the system because heavy vehicles can cause more structural damage.. All sensors have best results for method W1, which use only amplitude of peak up. Much more accurate results are achieved for heavy vehicles. Which is good news for practical application of the system because heavy vehicles can cause more structural damage.

Table 2 Weight estiamtion result comparison

Case	Category	Embedded_02						gfrp_01						gfrp_02					
		Absolute error [1000 kg]			Relative error [%]			Absolute error [1000 kg]			Relative error [%]			Absolute error [1000 kg]			Relative error [%]		
		MEAN	SD	VAR	MEAN	SD	VAR	MEAN	SD	VAR	MEAN	SD	VAR	MEAN	SD	VAR	MEAN	SD	VAR
W1	Trucks	0.2	1.2	1.5	5.5	4.4	19.6	0.2	1.8	3.1	7.3	6.7	45.4	0.1	1.0	1.0	4.3	4.2	17.7
	Cars&Other	-0.3	1.5	2.2	31.3	27.4	749.1	-0.2	1.1	1.2	29.8	38.8	1505.1	-0.2	1.3	1.6	29.3	28.5	811.5
	ALL	0.0	1.4	1.8	16.3	22.1	488.3	0.0	1.5	2.3	16.7	28.0	782.7	0.0	1.1	1.3	14.8	22.4	502.5
W2	Trucks	0.5	1.9	3.4	8.8	5.8	33.1	0.2	1.8	3.2	8.4	5.6	31.5	0.3	1.5	2.3	7.2	4.7	21.7
	Cars&Other	-0.6	2.0	4.2	40.0	51.8	2684.4	-0.2	1.4	1.8	28.4	38.5	1480.9	-0.4	1.8	3.1	34.6	45.2	2043.3
	ALL	0.0	2.0	4.1	22.0	37.2	1383.2	0.0	1.6	2.5	16.6	27.2	740.1	0.0	1.7	2.8	18.7	32.5	1056.0
W3	Trucks	0.4	1.8	3.4	8.0	7.1	49.8	0.3	2.0	3.9	9.1	6.6	43.6	0.1	0.9	0.8	4.1	3.3	10.8
	Cars&Other	-0.6	1.9	3.5	36.5	45.8	2098.2	-0.3	1.0	0.9	24.8	39.7	1572.6	-0.2	1.4	2.1	32.0	35.9	1288.6
	ALL	0.0	1.9	3.7	20.1	33.3	1108.3	0.0	1.7	2.8	15.8	27.3	745.2	0.0	1.2	1.4	15.8	27.2	737.8

5 Discussion

The scanning rate of FOS (10 Hz) is much lower than optimal scanning rate of typical BWIM systems (512Hz) [6]. The reason is that the primary purpose of the sensor system is SHM. Generally processed data from sensors Embedded_02 and gfrp_01 reported lower mean errors than gfrp_02. Similar results are observed for standard deviations (SD) except S2. The data set used to calculate statistical parameters had only around 90 points for weight and speed because WIM system ran only for a short period. Because of the limited number of data points the Calculation and validation were held on the same data set.

5.1 Results of speed estimation

The results (For results of measurement see For results of measurement see Table 1. Mean errors, standard deviations (SD) and variances (VAR) are presented. “All” category summarizes results of all data. Mean errors, standard deviations (SD) and variances (VAR) are presented. “All” category summarizes results of all data.) showed a systematic error of calculation methods S1 and S2. For the Trucks category the absolute mean error was positive and for Cars negative. For long vehicles, in the Trucks category, their length (17 m) is comparable to the bridge span length (23 m). The peak observed on the sensor also contains the vehicle’s length, and therefore the actual distance traveled is greater than that considered in calculation and that is why the speed is lower. The calculated absolute mean error according to (4) is therefore positive. For the Cars category, with a wheelbase of around 4 m, the actual distance contained in the peak duration is smaller and the speed is therefore larger. This dependence was corrected by linear regression in cases S3 and S4. The obtained coefficients of linear regression can be used to correct speed for the future measurements.The calculation using vehicle length as input parameter (from WIM) and following regression recalcualtion (S4) had similar errors like simple use of regression (S3).

5.2 Results of weight estimation

Available weight data were divided into two categories. Trucks and Cars&Other. Trucks with known weight 17800 kg and 18390 kg. Second group contains mainly Cars under 3500 kg and few vehicles under 8000 kg. Unfortunately, we had no samples between 8000 and 17000 kg because no vehicles passed the bridge during the day the measurement was realized. Weight error evaluation is limited.
Method W1 had best results. This metod uses only data from first bridge span, where are installed sensors. Methods W2 and W3 use amplitude from second span. This amplitude is obviously affected not only by the weight of passing vehicles but also by other influences (such as distribution of forces in the structure) and had negative effect on calculation preccision.Absolute errors and theirs SD for all categories were similar. Which, when comparing relative errors, means much better results for heavier vehicles.

6 Conclusion

We presented additional use for SHM FOS system installed on a road bridge. It has been shown that with presented simplified methods, the integrated FOS system is able to detect vehicle count, direction, estimate speed and weight of passing vehicles. Direction detection was 100 % reliable. Precision of calculated speed and weight is limited, but usable for traffic statistic.

Acknowledgement

This work is supported by project "Condition diagnostics and protection of bridge constructions system with application of WIM system" funded by Technology Agency of Czech Republic within program DOPRAVA 2020+.
Jan Vcelak gratefully acknowledges the European Commission for funding the InnoRenew CoE project (Grant Agreement no. 739574) under the Horizon2020 Widespread-Teaming program, and the Republic of Slovenia (Investment funding of the Republic of Slovenia and the European Union of the European Regional Development Fund).

References

[1] Zhao, H., Uddin, N.: Algorithm to identify axle weights for an innovative BWIM system- Part I, ABSE-JSCE Joint Conference on Advances in Bridge Engineering-II, Dhaka, Bangladesh, 8-10 August 2010.

[2] ZAG, Cestel, SiWIM Bridge Weigh-in-Motion Manual, 3rd Edition, May 2005, Slovenia

[3] Moses, F.: Weigh-in-motion system using instrumented bridges, Transportation Engineering Journal (ASCE), 105 (1979), pp. 233–249

[4] Moses, F., Verma, D.: Load Capacity Evaluation of Existing Bridges, National Cooperative Highway Research Program (NCHRP) Report 301, 1987, Washington D.C.

[5] Kalyankar, R., Uddin, N.: Axle detection on prestressed concrete bridge using bridgeweigh-in-motion system, J Civil Struct Health Monit, 7 (2017), pp. 191–205, DOI: 10.1007/s13349-017-0210-2

[6] Lydon, M., Robinson, D., Taylor, S.E., Amato, G., Brien, E.J.O., Uddin, N., Esveld, C.: Improved axle detection for bridge weigh-in-motion systems using fiber optic sensors, J Civil Struct Health Monit, 7 (2017), pp. 325–332, DOI: 10.1007/s13349-017-0229-4

[7] Capova, K., Velebil, L., Vcelak, J.: Laboratory and In-Situ Testing of Integrated FBG Sensors for SHM for Concrete and Timber Structures, Sensors, 20 (2020) 6, DOI: https://doi.org/10.3390/s20061661

[8] Capova, K., Velebil, L., Vcelak, J., Dvorak, M., Sasek, L.: Environmental Testing of a FBG Sensor System for Structural Health Monitoring of Building and Transport Structures, Procedia Structural Integrity, 17 (2019), pp. 726-733

[9] Grattan, S. K. T., Taylor, S.E., Muhammed Basheer, P.A.: Structural Health Monitoring - better solutions using fiber optic sensors, IEEE SENSORS 2009 Conference, New Zealand, 25-28 October 2009, DOI: 10.1109/ICSENS.2009.5398552

[10] Fibre Bragg grating sensors, Safibra s.r.o., http://www.safibra.cz/, 11.3.2022

[11] RAO, Y.J.: In-fibre Bragg grating sensors. Measurement Science and Technology. IOP Publishing, 8 (1997) 4, pp. 355-375, DOI: 10.1088/0957-0233/8/4/002

[12] Weight in motion system, Camea, https://www.camea.cz/cz/doprava/vazeni-za-jizdy-wim/, 11.3.2022

[13] Bernard, J., O'Brien, E., Jehaes, S.: Weigth-in-Motion of Road Vehicles: European WIM specification, Paris: Laboratoire Central des Ponts et Chaussées, 2002.